

Adaptive Exponentially Weighted Extended Kalman Filtering for State of Charge Estimation of Lithium-ion Battery

Jin Li, Shunli Wang^{}, Lei Chen, Mingfang He*

School of Information Engineering, Southwest University of Science and Technology, Mianyang 621010, China;

*E-mail: 497420789@qq.com

Received: 12 September 2021 / *Accepted:* 1 November 2021 / *Published:* 6 June 2022

When implementing Kalman filtering on a nonlinear system, it is necessary to expand its Taylor expansion and discard the terms above the second-order to realize the application expansion on the nonlinear system. Based on the establishment of a second-order RC circuit equivalent model, the parameters of the lithium-ion battery are identified, combined with the extended Kalman filter. However, the extended Kalman filter has the disadvantage of assuming that the noise is fixed, which reduces the correlation between the noise and the prediction, and finally produces the effect of filtering divergence. Therefore, the noise evaluation standard is set through the exponentially weighted average, and the noise is continuously adjusted to achieve filter convergence and improve estimated accuracy. Getting the simulation on the MATLAB and in the experiments of various working conditions, the average error of SOC estimation was within 1.5%, and the highest error was within 4%.

Keywords: extended Kalman filter; adaptive strategy; exponentially weighted average

1. INTRODUCTION

The energy problem is one of the most severe survival problems faced by mankind in the 21st century. There is not only the environmental pollution caused by fossil energy but also the shortage of non-renewable energy. Therefore, the development of new energy has become the common pursuit of the world. Electric energy[1], as an environmentally friendly new energy source, is emerging in new energy sources. Lithium-ion batteries, as an important energy storage medium for electric energy, it has the advantages of portable and high specific energy, 2.5 times that of ordinary zinc-manganese batteries[2], high specific power, and can discharge and discharge at large currents. With the advantages of stable current, it also is recyclable and long life, lithium-ion batteries are widely used in new energy equipment. And grasping the estimation of the State of Charge (SOC)[3] of the lithium-ion battery is

conductive to fully understand the working state of the lithium-ion battery so that the lithium-ion battery can be used rationally[4], and the damage to the battery can be reduced. So, how to establish corresponding equivalent models for the working characteristics of different lithium-ion batteries and use different algorithms to analyze and calculate their SOC has become the current research focus[5].

There are many methods used to estimate the SOC of lithium-ion batteries. The traditional method: (1) Discharge test method[6]: However, the test process of this method takes a lot of time, when using this method, the target battery needs to be removed from the electric vehicle[7], so the method cannot be used to calculate the power battery in working condition. (2) Ampere-hour integration method[8]: This method only uses the external characteristics of the battery as the basis for SOC estimation. To a certain extent, it ignores the influence of battery self-discharge rate, aging degree, and charge-discharge rate on battery SOC. Long-term use will also lead to measurement, the error continues to accumulate and expand, so it is necessary to introduce relevant correction coefficients to correct the accumulated error. (3) Open-circuit voltage method[9]: the target battery must be allowed to stand for more than 1h before measuring OCV to obtain a stable terminal voltage in this method. These methods have a simple foundation and a single implementation process, which often leads to low estimation accuracy or low versatility. (4) Kalman filtering[10]: In the 1960s, the American mathematician R.E.Kalman proposed a new type of optimal autoregressive data filtering algorithm, using the principle of minimum mean square error to make the best estimation of the state of complex dynamic systems[11]. When the Kalman filter method is used to estimate the SOC of a power battery, the battery is transformed into a state-space model in the form of a power system[12], and the SOC becomes a state variable inside the model. However, the Kalman filter is only for linear systems[13], and the operating characteristics of the lithium-ion battery itself present a high degree of non-linearity. In order to apply the Kalman filter to the SOC estimation of the lithium-ion battery, Plett[14] established the equivalent model of the lithium-ion battery circuit based on Extended Kalman Filter (EKF)[15] is applied in the estimation of SOC of the lithium-ion battery, which can solve the nonlinear first-order system. The extended Kalman filter is a Taylor expansion[16] of the Kalman filter, discarding the second-order and above terms and realizing the expansion of the application of the Kalman filter in nonlinearity.

The above methods are more and more accurate for lithium-ion battery SOC estimation, but they ignore the relationship and change of noise in iteration and SOC in the noise processing[17]. This paper is based on the EKF algorithm, according to the random distribution of noise in the algorithm, strengthens the adjustment of noise in algorithm prediction. The noise adjustment coefficient is added by using the exponential weighting method to realize the update of the noise in each iteration, achieve the adaptive adjustment of the noise covariance, further increase the estimation accuracy, and realize the Exponential Weighted Adaptive Extended Kalman Filter (AEW-EKF).

2. THEORETICAL ANALYSIS

2.1. The second-order RC equivalent circuit modeling

The battery equivalent model has a significant impact on the accuracy of battery SOC estimation, and there are many models widely used now, including the Thevenin model[7] which only considers the

rapid changes in polarization response of the battery. Rint[18] model is a simple model which does not consider the polarization characteristics of battery, so its accuracy is not ideal. PNGV[19] model has high accuracy in simulating transient response and is suitable for high current step type and complex charging and discharging conditions, but not for this article's condition. Taking into account the non-linear voltage change and calculation amount caused by the internal chemical reaction of the battery, the second-order RC equivalent model[20] is the best choice compared with above several models. The second-order RC equivalent model is shown in Figure 1:

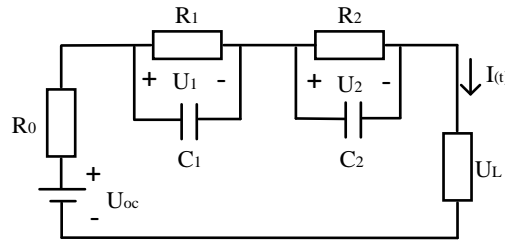


Figure 1. Equivalent circuit model

Fig. 1, U_{oc} represents the open-circuit voltage, U_L represents the terminal voltage. R_1 and R_2 are the polarization resistances, C_1 and C_2 are the polarization capacitances. R_1 and C_1 represent the rapid change phase of the internal voltage[21] of the battery, R_2 and C_2 represent the slow change phase of the internal voltage of the battery. The second-order model is simple, easy to calculate, and the accuracy is high. The higher-order model has little improvement in accuracy but the amount of calculation is significantly increased, so the second-order model is the best choice for this research. According to Kirchhoff's law[22], Eq. (1) can be obtained in conjunction with Fig. 1.

$$\begin{cases} U_{oc} = I_{(t)}R_0 + U_1 + U_2 + U_L \\ \frac{dU_1}{dt} = -\frac{U_1}{R_1C_1} + \frac{I}{C_1} \\ \frac{dU_2}{dt} = -\frac{U_2}{R_2C_2} + \frac{I}{C_2} \end{cases} \quad (1)$$

According to the second-order RC model, with $[SOC \ U_1 \ U_2]$ as the state variable, combining Eq. (1) and SOC definition Eq. (2), the state space Eq. (3) is obtained after discretization[23].

$$SOC_t = SOC_0 - \frac{\int_0^t I_{(t)} \eta dt}{C} \quad (2)$$

$$\begin{bmatrix} SOC_{k+1} \\ U_{1,k+1} \\ U_{2,k+1} \end{bmatrix} = \begin{bmatrix} 1 & 0 & 0 \\ 0 & e^{-\frac{\Delta t}{\tau_1}} & 0 \\ 0 & 0 & e^{-\frac{\Delta t}{\tau_1}} \end{bmatrix} \begin{bmatrix} SOC_k \\ U_{1,k} \\ U_{2,k} \end{bmatrix} + \begin{bmatrix} -\frac{\Delta t}{Q_N} \\ R_1(1-e^{-\frac{T}{\tau_1}}) \\ R_2(1-e^{-\frac{T}{\tau_2}}) \end{bmatrix} I_k + w_k \quad (3)$$

$$U_{L,k+1} = U_{oc,k} - R_{0,k} I_k - [0 \quad -1 \quad -1] \begin{bmatrix} SOC_k \\ U_{1,k} \\ U_{2,k} \end{bmatrix} + v_k \quad (4)$$

Among them, w_k and v_k are Gaussian white noise, the former represents the state error, and the latter represents the measurement error. Q_N is the rated power of the battery, and Δt is the sampling interval, $\tau = RC$ [24].

2.2. Parameter identification

According to Eq. (3), the parameters that need to be identified through parameter identification in the model are ohmic internal resistance R_0 , open circuit voltage U_{oc} , polarization resistance R_1 , R_2 , and polarization capacitance C_1 , C_2 . The ternary lithium-ion battery was selected for the Hybrid Pulse Power Characterization (HPPC) experiment[25]. The nominal capacity of the battery was 45Ah and the actual capacity was 44.36Ah. The HPPC experiment was carried out at a constant temperature of 27°C. Fig. 2 shows a cycle of the HPPC experiment.

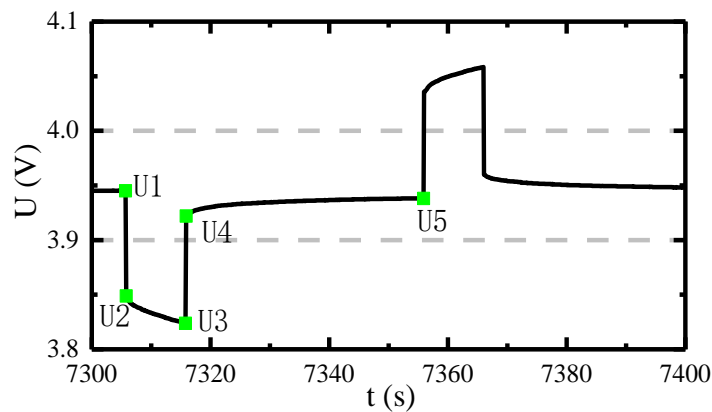


Figure 2. One pulse experimental voltage curve when SOC=0.7

According to Fig. 2, it can be seen that the stages U_1 to U_2 and the stages U_3 to U_4 are affected by the ohmic resistance at the beginning and the end of the discharge, the ohmic resistance is obtained as Eq. (5).

$$R_0 = \frac{|U_1 - U_2| + |U_4 - U_3|}{2I} \quad (5)$$

The slow rise of voltage from U_4 to U_5 is the zero-input stage of the two RC loops, and there is no current in the power supply at this stage. Therefore, the terminal voltage Eq. (6) can be obtained.

$$U_L = U_{oc} - IR_1 e^{-\frac{t}{\tau_1}} - IR_2 e^{-\frac{t}{\tau_2}} \quad (6)$$

2.3. Exponentially Weighted Adaptive Extended Kalman filter

Kalman filter is an optimized autoregressive[26] data processing algorithm that improves the accuracy of lithium-ion battery SOC estimation by optimally estimating state variables. The form of Kalman filter state equation[27] and observation equation[27] are as Eq. (7).

$$\begin{cases} x_{k+1} = f(x_k, k) + w_k \\ y_k = h(x_k, k) + v_k \end{cases} \quad (7)$$

The first-order Taylor expansion[28] of the Kalman filter ignoring the second-order and above terms, realizes the conversion of nonlinear problems into linear problems for processing, then defining A_k , B_k , C_k , and D_k , as Eq. (8), (9), and (10).

$$\begin{cases} f(x_k, k) \approx f(\hat{x}_k, k) + \left. \frac{\partial f(x_k, k)}{\partial x_k} \right|_{x_k = \hat{x}_k} (x_k - \hat{x}_k) \\ h(x_k, k) \approx h(\hat{x}_k, k) + \left. \frac{\partial h(x_k, k)}{\partial x_k} \right|_{x_k = \hat{x}_k} (x_k - \hat{x}_k) \end{cases} \quad (8)$$

$$\begin{cases} A_k = \left. \frac{\partial f(x_k, k)}{\partial x_k} \right|_{x_k = \hat{x}_k} \\ B_k = f(\hat{x}_k, k) - A_k \hat{x}_k \\ C_k = \left. \frac{\partial h(x_k, k)}{\partial x_k} \right|_{x_k = \hat{x}_k} \\ D_k = h(\hat{x}_k, k) - C_k \hat{x}_k \end{cases} \quad (9)$$

$$\begin{cases} x_{k+1} = A_k x_k + B_k u_k + \omega_k \\ y_k = C_k x_k + D_k + v_k \end{cases} \quad (10)$$

Before performing the extended Kalman filter, it is necessary to initialize the initial state value x_0 and the error covariance[29] P_0 , as shown in formula (11):

$$\begin{cases} \hat{x}_0 = E[X_0] \\ P_0 = E[X_0 - \hat{x}_0 (X_0 - \hat{x}_0)^T] \end{cases} \quad (11)$$

AEW-EKF algorithm adds an adjustment coefficient[30] for noise base on EKF so that each iteration in the filtering can adjust the noise according to the previous prediction error and improve the accuracy. Actually, the noise environment in which the lithium-ion battery is located cannot be just white noise. Adjusting the noise means[31] square error can better simulate the actual situation. The steps of AEW-EKF are as follows:

The first is the state prediction as Eq. (12), then the prediction covariance P is as Eq. (13), combined with the prediction covariance to calculate the Kalman gain K [32] as Eq. (14), and finally, the prediction result and covariance are updated by the Kalman gain as Eq. (15) and (16).

$$\hat{x}(k | k - 1) = A(k)\hat{x}(k - 1) + B(k)I(k - 1) \tag{12}$$

$$P(k | k - 1) = A(k - 1)P(k - 1)A^T(k - 1) + Q / \mu_k \tag{13}$$

$$K(k + 1) = P(k | k - 1)C^T(k)[C(k)P(k | k - 1)C^T(k)] + \mu_k R \tag{14}$$

$$\hat{x}(k) = \hat{x}(k | k - 1) + K(k)[v(k) - \hat{v}(k)] \tag{15}$$

$$P(k) = [I - K(k)C(k)]P(k | k - 1) \tag{16}$$

The μ in equations (13) and (16) is the adjustment coefficient. The noise covariance is adjusted in the covariance prediction and Kalman gains calculation. The specific ideas are as follows:

Defining $Err(k)$ represents the error between the SOC predicted value and the actual value calculated in each iteration, and $sum(k)$ represents the sum of the absolute value of the error after each iteration. In a time-varying system[33], recent data has a greater impact on the system, so the exponential weighted average method is used when measuring the impact of errors on the system. This method controls the influence of the error on the judgment basis $judge(k)$ by setting the weighting coefficient β .

$$judge(k) = \beta \cdot judge(k - 1) + (1 - \beta) \cdot \left(\frac{\sum_{i=1}^{k-1} Err(i)}{k - 1} + abs(Err(k)) \right) \tag{17}$$

Eq. (17) is the judgment standard $judge(k)$. Using the judgment standard to evaluate the error of each iteration, and set the adjustment coefficient μ to adjust the noise in the next iteration, as in Eq. (18):

$$\mu_k = \begin{cases} \frac{abs(Err(k))}{judge(k)} & judge(k) > abs(Err(k)) \\ 1 & judge(k) \leq abs(Err(k)) \end{cases} \tag{18}$$

In repeated iterations, the earlier error data plays a smaller role in this adaptation[34], and the previous error data has the greatest impact on this error, which improves the correlation between the data and makes the result more accurate.

The flow chart of the AEW-EKF algorithm is shown in Fig. 3:

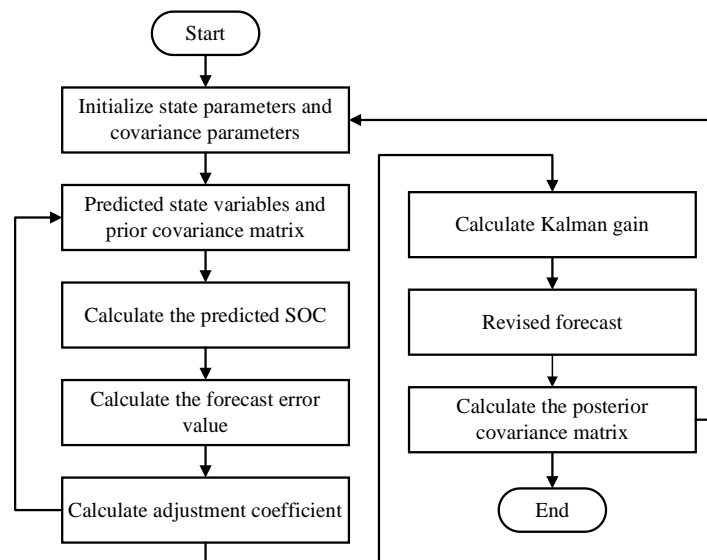


Figure 3. AEW-EKF algorithm flow chart

3. IDENTIFICATION RESULT

Through the parameter identification of the experimental data, the model parameters of different SOC stages can be obtained, including: ohmic resistance R_0 , open circuit voltage U_{oc} , polarization resistance R_1, R_2 and polarization capacitance C_1, C_2 , as shown in Tab. 1:

Table 1. Model parameter of each SOC state

SOC	$R_0/m\Omega$	U_{oc}/V	$R_1/m\Omega$	$R_2/m\Omega$	C_1/F	C_2/F
1	2.1718	4.1840	0.1699	0.7878	2896.90651	19692.26783
0.9	2.1921	4.0556	0.1639	0.8833	2858.700248	18637.74289
0.8	2.1864	3.9450	0.1560	0.9171	3103.026753	17553.55079
0.7	2.1787	3.8433	0.1644	0.9536	2857.376163	16582.87125
0.6	2.1787	3.7366	0.1403	0.8225	3555.416636	16634.82359
0.5	2.1710	3.6551	0.0986	0.5426	4710.637546	19439.1881
0.4	2.1651	3.6157	0.1014	0.5715	4947.320054	21896.43719
0.3	2.1821	3.5822	0.1301	0.8564	4395.921333	25350.40817
0.2	2.2023	3.5199	0.1229	0.8115	4272.714207	20680.43146
0.1	2.2618	3.4396	0.1379	0.8350	4197.630901	14071.08682

According to Tab. 1, the model parameters will change with the change of SOC value. It is obvious that the relationship between SOC and each parameter is not a simple linear relationship[35], so in order to achieve accurate simulation, it is necessary to pass multiple fittings. Ways to find the relationship between each parameter and SOC.

4. SIMULATION RESULTS

4.1. Parameter verification based on HPPC test

In order to verify the feasibility of the AEW-EKF algorithm and the accuracy of parameter identification[36], a second-order RC lithium-ion battery equivalent model[37] was constructed in Simulink/MATLAB for experimental simulation[38] and the results are shown in Fig. 4:

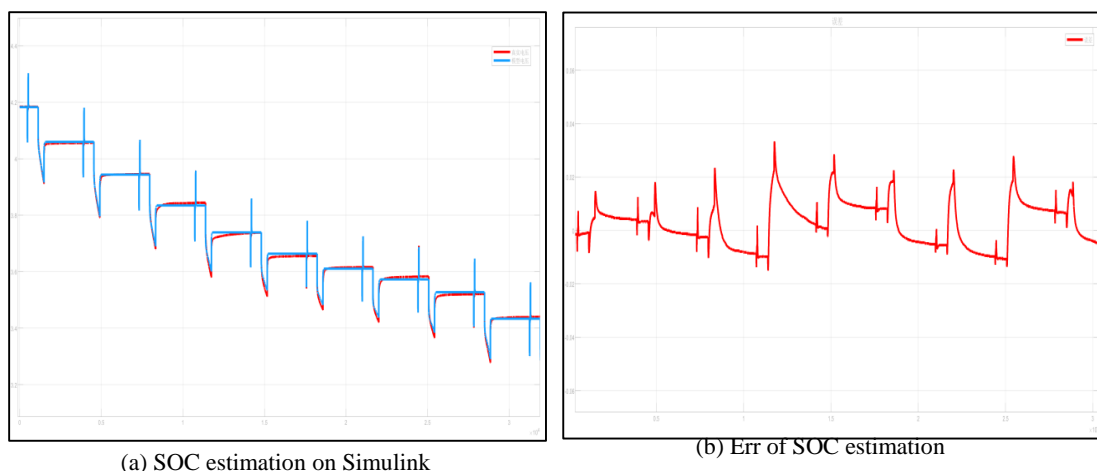


Figure 4. Simulation and error of SOC estimation under HPPC Test in Simulink

It can be seen from Fig. 4 (a) that the calculation of the second-order RC equivalent model parameters is accurate, and the experimental value[39] and the estimated value curve fit very well. According to Fig.4 (b), the maximum error is 0.03332, and the accuracy reaches 96.668%. The result of parameter identification is very ideal, and it can be used in the AEW-EKF algorithm to estimate SOC.

4.2. AEW-EKF based on DST condition experiment

To further verify the ability of the AEW-EKF algorithm to estimate the state of charge of lithium-ion batteries under complex working conditions, it was decided to test the feasibility of the algorithm through the Dynamic Stress Test (DST)[40]. It is verified by Beijing Bus Dynamic Stress Test (BBDST)[41] and compared with the EKF algorithm and SOC reference value under the same working conditions.

According to the real data collection of Beijing buses to get the working conditions, and it can be calculated that the single cycle time is 300s. Using the experimental equipment to set the process steps until the battery runs out, collecting the experimental data, and using the AEW-EKF and EKF algorithms to estimate the SOC, then comparing with the reference value. The comparison diagram and the partially enlarged diagram are shown in Figure 5:

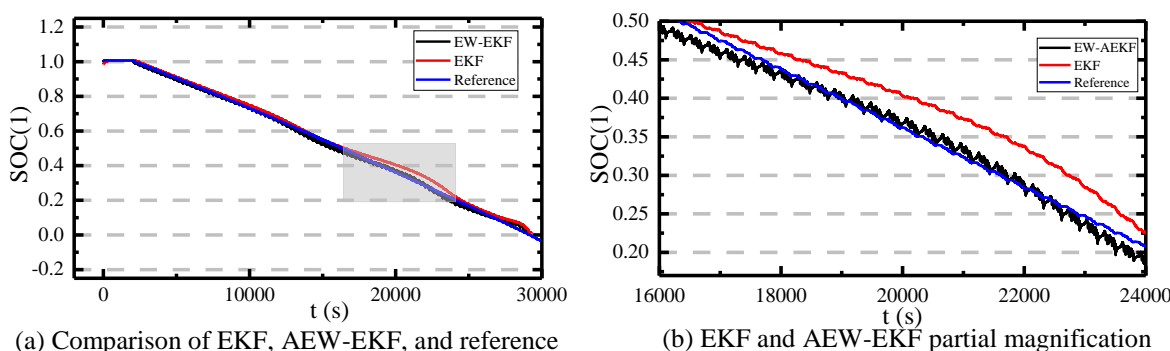


Figure 5. Estimation and error comparison under BBDST conditions

It can be seen from Fig. 5 that both the EKF and AEW-EKF algorithms have a good follow-up effect on the reference value. The black curve is the SOC estimation result of the EKF algorithm, and the red is the change result of the AEW-EKF algorithm after exponentially weighted adaptation. It can be seen from Fig. 5 (b) that the result of AEW-EKF is closer to the reference value than EKF. At the same time, the curve of EKF has more burrs and is more affected by noise, while the curve of the AEW-EKF algorithm is smoother, indicating an ideal effect on noise processing.

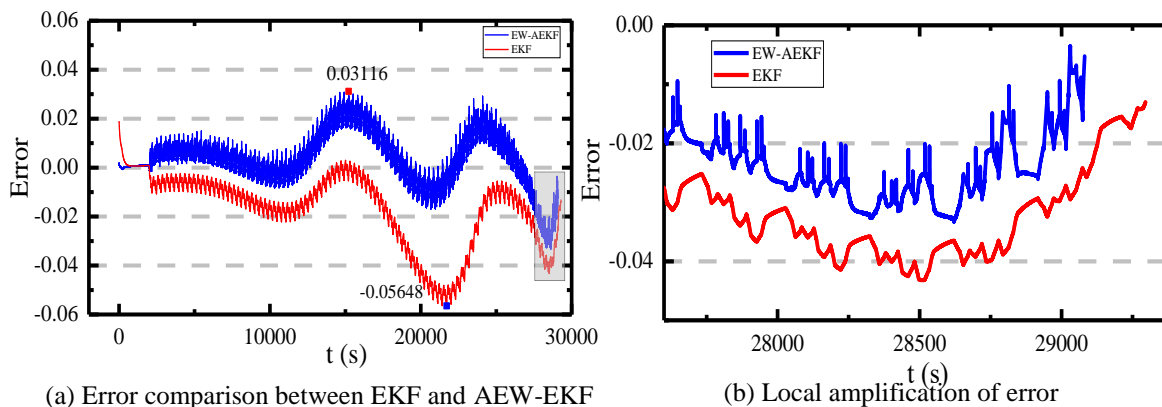


Figure 6. Comparison of SOC estimation error obtained by EKF and AEW-EKF

Fig. 6 is the error comparison and partial enlargement of the EKF algorithm and the AEW-EKF algorithm. In the whole process, although the AEW-EKF algorithm cannot be consistently better than EKF, from the error point of view, the average error of AEW-EKF is about 0.83%, the maximum error is 3.12%, the average error of the EKF algorithm is 1.74%, and the maximum error is 5.65%. It can be seen that the SOC estimation after the adaptive strategy has a certain correction effect relative to the EKF algorithm, which improves the accuracy.

5. CONCLUSIONS

The second-order RC circuit equivalent model used in this paper can better represent the parameter changes caused by the internal chemical changes in the working state of the lithium-ion battery. Through parameter identification and simulation can verify the accuracy of the model. On this basis, making estimation for SOC of lithium-ion battery. Aiming at the defects of the extended Kaiman filter algorithm, this paper performs exponential weighting processing on the result error of each prediction iteration and adaptively integrates it into the filter algorithm to make the previous iteration error's weight is closer to this prediction, which improves the accuracy of the algorithm. Comparing the results of EKF with AEW-EKF, it can be proved that the adaptively adjusted EKF algorithm can better estimate the SOC, and the average estimation error is reduced by 0.91%, which is beneficial to better strengthen the management of the battery.

References

1. Z. Ren, C. Du, H. Wang and J. Shao, *International Journal of Electrochemical Science*, 15 (2020) 9981.
2. C. Lin, Q. Yu, R. Xiong and L. Y. Wang, *Applied Energy*, 205 (2017) 892.
3. L. Wu, K. Liu, H. Pang and J. Jin, *Energies*, 14 (2021) 5262.
4. G. S. Misyris, D. I. Doukas, T. A. Papadopoulos, D. P. Labridis and V. G. Agelidis, *Ieee Transactions on Energy Conversion*, 34 (2019) 109.
5. L. Hu, X. Hu, Y. Che, F. Feng, X. Lin and Z. Zhang, *Applied Energy*, 262 (2020) 114569.
6. S. Li, M. Hu, Y. Li and C. Gong, *International Journal of Energy Research*, 43 (2019) 417.
7. X. Lai, S. Wang, L. He, L. Zhou and Y. Zheng, *Journal of Energy Storage*, 27 (2020) 101106.
8. Y. Li, G. Xu, B. Xu and Y. Zhang, *International Journal of Electrochemical Science*, 16 (2021) 151050.
9. Y. Xu, M. Hu, C. Fu, K. Cao, Z. Su and Z. Yang, *Electronics*, 8 (2019) 1012.
10. Y. Xu, M. Hu, A. Zhou, Y. Li, S. Li, C. Fu and C. Gong, *Applied Mathematical Modelling*, 77 (2020) 1255.
11. J. Hou, Y. Yang, H. He and T. Gao, *Applied Sciences-Basel*, 9 (2019) 1726.
12. B. Zhao, J. Hu, S. Xu, J. Wang, Y. Zhu, L. Zhang and C. Gao, *Ieee Access*, 8 (2020) 198706.
13. G. Jin, L. Li, Y. Xu, M. Hu, C. Fu and D. Qin, *Energies*, 13 (2020) 1785.
14. W. Wang, X. Wang, C. Xiang, C. Wei and Y. Zhao, *Ieee Access*, 6 (2018) 35957.
15. D. N. T. How, M. A. Hannan, M. S. H. Lipu and P. J. Ker, *Ieee Access*, 7 (2019) 136116.
16. C. Chen, R. Xiong, R. Yang, W. Shen and F. Sun, *Journal of Cleaner Production*, 234 (2019) 1153.
17. B. Jiang, H. Dai, X. Wei and T. Xu, *Applied Energy*, 253 (2019) 113619.
18. J. Li, M. Ye, S. Jiao, W. Meng and X. Xu, *Ieee Access*, 8 (2020) 185629.
19. Y. Liu, T. Cai, J. Liu, M. Gao and Z. He, *Journal of Electrical Engineering & Technology*, 15 (2020) 2529.
20. S. Liu, N. Cui and C. Zhang, *Energies*, 10 (2017) 1345.
21. H.-Y. Long, C.-Y. Zhu, B.-B. Huang, C.-H. Piao and Y.-Q. Sun, *Journal of Electrical Engineering & Technology*, 14 (2019) 1485.
22. X. Lu, H. Li, J. Xu, S. Chen and N. Chen, *Energies*, 11 (2018) 714.
23. S. Mendoza, J. Liu, P. Mishra and H. Fathy, *Journal of Energy Storage*, 11 (2017) 86.
24. J. Meng, M. Ricco, G. Luo, M. Swierczynski, D.-I. Stroe, A.-I. Stroe and R. Teodorescu, *Ieee Transactions on Industry Applications*, 54 (2018) 1583.
25. H. S. Ramadan, M. Becherif and F. Claude, *International Journal of Hydrogen Energy*, 42 (2017) 29033.
26. C. Zhang, J. Jiang, L. Zhang, S. Liu, L. Wang and P. C. Loh, *Energies*, 9 (2016) 900.
27. P. Saha, S. Dey and M. Khanra, *Journal of Power Sources*, 434 (2019) 226696.
28. S. Ressel, F. Bill, L. Holtz, N. Janshen, A. Chica, T. Flower, C. Weidlich and T. Struckmann, *Journal of Power Sources*, 378 (2018) 776.
29. A.-I. Shoe, J. Meng, D.-I. Shoe, M. Swierczynski, R. Teodorescu and S. K. Kaer, *Energies*, 11 (2018) 795.
30. J.-N. Shen, J.-J. Shen, Y.-J. He and Z.-F. Ma, *Ieee Transactions on Power Electronics*, 34 (2019) 4329.
31. P. Shrivastava, T. K. Soon, M. Y. I. Bin Idris and S. Mekhilef, *Renewable & Sustainable Energy Reviews*, 113 (2019) 109233.
32. Q. Wang and W. Qi, *Journal of Power Electronics*, 20 (2020) 614.
33. Q. Wang, J. Wang, P. Zhao, J. Kang, F. Yan and C. Du, *Electrochimica Acta*, 228 (2017) 146.
34. Q. Yu, R. Xiong, C. Lin, W. Shen and J. Deng, *Ieee Transactions on Vehicular Technology*, 66 (2017) 8693.

35. X. Wu, X. Li and J. Du, *Ieee Access*, 6 (2018) 41993.
36. Z. Xi, M. Dahmardeh, B. Xia, Y. Fu and C. Mi, *Ieee Transactions on Vehicular Technology*, 68 (2019) 8613.
37. S. Yang, C. Deng, Y. Zhang and Y. He, *Energies*, 10 (2017) 1560.
38. J. Yang, B. Xia, Y. Shang, W. Huang and C. C. Mi, *Ieee Transactions on Vehicular Technology*, 66 (2017) 10889.
39. Z. Zeng, J. Tian, D. Li and Y. Tian, *Energies*, 11 (2018) 59.
40. B. Xia, Z. Lao, R. Zhang, Y. Tian, G. Chen, Z. Sun, W. Wang, W. Sun, Y. Lai, M. Wang and H. Wang, *Energies*, 11 (2018) 3.
41. J. Xie, J. Ma and K. Bai, *Journal of Power Electronics*, 18 (2018) 910.

© 2022 The Authors. Published by ESG (www.electrochemsci.org). This article is an open access article distributed under the terms and conditions of the Creative Commons Attribution license (<http://creativecommons.org/licenses/by/4.0/>).